

A Maximum Likelihood Analysis of the Low CMB Multipoles from WMAP

G. Efstathiou

Institute of Astronomy, Madingley Road, Cambridge, CB3 0HA.

29 November 2018

ABSTRACT

The amplitudes of the quadrupole and octopole measured from the Wilkinson Microwave Anisotropy Probe (WMAP) appear to be lower than expected according to the concordance Λ CDM cosmology. However, the pseudo- C_ℓ estimator used by the WMAP team is non-optimal. In this paper, we discuss the effects of Galactic cuts on pseudo- C_ℓ and quadratic maximum likelihood estimators. An application of a quadratic maximum likelihood estimator to Galaxy subtracted maps produced by the WMAP team and Tegmark, de Oliveira-Costa and Hamilton (2003) shows that the amplitudes of the low multipoles are stable to different Galactic cuts. In particular, the quadrupole and octopole amplitudes are found to lie in the ranges $\Delta T_2^2 = 176 - 250 (\mu K)^2$ and $\Delta T_3^2 = 794 - 1183 (\mu K)^2$ (and more likely to be at the upper ends of these ranges) rather than the values $\Delta T_2^2 = 123 (\mu K)^2$ and $\Delta T_3^2 = 611 (\mu K)^2$ found by the WMAP team. These results indicate that the discrepancy with the concordance Λ CDM model at low multipoles is not particularly significant and is in the region of a few percent. This conclusion is consistent with an analysis of the low amplitude of the angular correlation function computed from quadratic maximum likelihood power spectrum estimates.

Key words: cosmic microwave background, cosmology.

1 INTRODUCTION

Over the last decade or so, a wide range of astronomical data has suggested that our Universe is described by a ‘concordance’ Λ CDM model (see *e.g.* Bahcall *et al.* 1999; Wang *et al.* 2002). According to this model, the Universe is spatially flat and dominated by vacuum energy density and weakly interacting cold dark matter. In addition, the primordial fluctuations are nearly scale invariant, as predicted in simple inflationary models of the early Universe. The beautiful observations of the cosmic microwave background (CMB) anisotropies made by the WMAP satellite have added strong support for this model (Bennett *et al.* 2003a; Spergel *et al.* 2003, hereafter S03).

However, the quadrupole and (to a lesser extent) the octopole amplitudes measured by WMAP are lower than expected according to the best fitting Λ CDM model (Bennett *et al.* 2003a; S03). The discrepancy at low multipoles was quantified by S03, who estimated that the lack of structure at angular scales $\theta > 60^\circ$ on the CMB sky would occur by chance with a probability of only 1.5×10^{-3} if the concordance Λ CDM model is correct. This striking result has stimulated a lot of interest, since it might indicate the need for exotic new physics (see *e.g.* Efstathiou 2003a; Contaldi *et al.* 2003; Cline, Crotty and Lesgourgues 2003; Feng and Zhang 2003; DeDeo, Caldwell and Steinhardt 2003).

However, a number of authors have questioned S03’s estimate of the statistical significance of the discrepancy. Tegmark, de Oliveira-Costa and Hamilton (2003, hereafter TdOH03) constructed an all-sky Galaxy subtracted map from the WMAP data and derived higher amplitudes for the octopole and quadrupole, concluding that the discrepancy is much less significant (in the region of a few percent). Efstathiou (2003b, hereafter E03b) argues that errors caused by inaccurate subtraction of Galactic emission (ignored by S03) should be folded into the error budget of the low multipoles and that these reduce the discrepancy to the level of a few percent. Other authors have applied Bayesian statistics (rather than the frequentist statistics discussed by S03) to test whether modified models, *e.g.* with a sharp break in the power spectrum on large spatial scales, are preferred to the concordance Λ CDM cosmology (*e.g.* Bridle *et al.* 2003; Cline *et al.* 2003; Contaldi *et al.* 2003; Niarchou *et al.* 2003). Although the Bayesian analyses generally favour some modification, they do not strongly exclude the simple concordance Λ CDM model. A comparison of frequentist and Bayesian statistics applied to the low CMB multipoles is given by E03b and will not be discussed further in this paper.

In a previous paper (E03b) I pointed out that the WMAP analysis of the CMB power spectrum (and angular correlation function) used a pseudo- C_ℓ (hereafter PCL) estimator (Hinshaw *et al.* 2003). This type of estimator

arXiv:astro-ph/0310207v2 1 Mar 2004

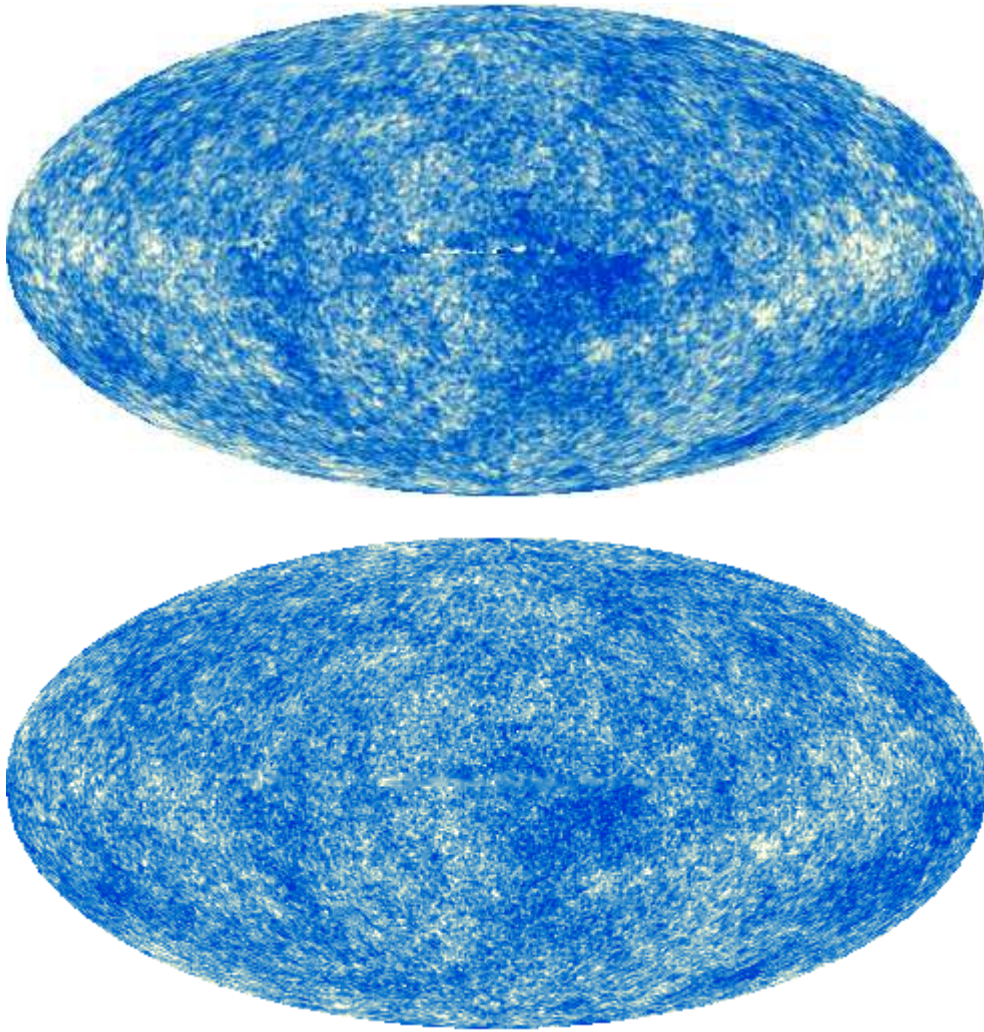


Figure 1. The upper figure shows the WMAP-ILC map of Bennett *et al.* (2003b) which is smoothed with a Gaussian beam of 1° FWHM. The lower figure shows the Wiener filtered component separated map of TdOH03.

has been discussed extensively in the literature (see Peebles 1973; Wandelt, Hivon and Górski 2001; Hivon *et al.* 2002; Efstathiou 2003c, hereafter E03c) and is known to be non-optimal if applied to an incomplete map of the sky. I also pointed out that a quadratic maximum likelihood (hereafter QML) estimator (see Tegmark 1997, E03c) can return *almost the exact values* for the low CMB multipoles from an incomplete map of the sky, provided that the sky cut is not too large and instrumental noise is negligible (a good approximation for WMAP at large angular scales). It could be argued, with some justification, that for the relatively modest Galactic cuts that have been applied to the WMAP data, the type of estimator used to assess the statistical significance of the low multipoles should not be particularly critical. For example, if a PCL estimator is applied with a particular sky cut, the results can be compared with simulated data using the same estimator and sky cut (exactly this type of comparison has been done by S03 and E03b). However, the real CMB sky contains emission from the Galaxy. As we vary the Galactic cut, how can we tell whether small changes in the low CMB multipoles are caused by inaccuracies in Galactic emission or by the effects of the sky cut on the estimator? This is where a QML estimator can help,

since the low CMB multipoles should be stable to the Galactic cut if a QML estimator is applied to the data.

As the low CMB multipoles have stimulated so much theoretical interest, it is surely important to make the most accurate estimates possible of their amplitudes from the WMAP data, and to test their sensitivity to residual Galactic emission. This is the aim of this paper.

The performance of PCL and QML estimators for different sky cuts is discussed in Section 2 and tested against numerical simulations. In Section 3, the QML and PCL estimators are then applied to Galaxy subtracted maps produced by the WMAP team (Bennett *et al.* 2003b, hereafter B03b) and by TdOH03 (see Figure 1). Section 4 describes an analysis of the S statistic defined by S03 (equation 10 below). The conclusions are summarized in Section 5.

2 POWER SPECTRUM ESTIMATORS AND INPUT MAPS

2.1 Contributions to the Error Budget and Input Maps

The error budget of an estimator of the CMB power spectrum can be broken down into four contributions:

(i) At low multipoles, the largest source of error is usually cosmic variance, which depends on the true form of the ensemble average of the CMB power spectrum, C_ℓ . For full sky coverage, the cosmic variance is given by the well known formula

$$\langle \Delta C_\ell^2 \rangle = \frac{2C_\ell^2}{(2\ell + 1)}. \quad (1)$$

(ii) Next, there is an error associated with the particular estimator used to evaluate the power spectrum. For example, if a PCL estimator is used to estimate the power spectrum over a cut sky, the estimates will differ from the actual values for our particular realization of sky since the cut introduces a loss of information. We will call this source of error ‘estimator induced variance’. It is sometimes represented, heuristically, by dividing equation (1) by f_{sky} , where f_{sky} is the fraction of the area of the sky that is unmasked.

(iii) Instrumental noise will increase the errors above the cosmic variance limit of equation (1). For WMAP, instrumental noise is unimportant at low multipoles and so will be ignored in the rest of this paper.

(iv) Systematic errors from various sources will add to the variance. For the WMAP data at low multipoles, the most important source of systematic error is residual contamination from the Galaxy (B03b; Hinshaw *et al.* 2003).

Cosmic variance is an irreducible component of the error budget. Accordingly, in this paper we concentrate on estimator induced variance and systematic errors and ask what are the best estimates of the amplitudes of the low CMB multipoles for our particular realisation of the sky?

The effects the Galaxy can be removed by exploiting the frequency dependence of Galactic emission. This has been used by B03b to produce a internal linear combination map (henceforth referred to as the ‘WMAP-ILC’ map) of the CMB anisotropies, from which the Galaxy has been subtracted. This map is plotted in the upper panel of Figure 1. A similar linear combination map, but using the component separation method of Tegmark and Efstathiou (1996), has been produced by TdOH03. This map (hereafter referred to as the ‘TdOH03’ map) is plotted in the lower panel of Figure 1. The reader is referred to the papers of B03b and TdOH03 for details of how these maps were produced.

The low order CMB multipoles can be evaluated from these maps without imposing a sky cut (TdOH03), in which case the question of estimator induced variance does not arise since all 4π steradians of sky are used. However, it is obvious from visual inspection of Figure 1 that the Galactic subtraction is not perfect (see also Figure 4), and hence one might worry about the extent to which the low CMB multipoles are affected by inaccurate Galactic subtraction. One way of reducing the effects of Galactic emission still further is by applying a sky cut. However, as the sky cut

is made larger, the estimator induced variance will generally increase. The main goal of this paper is to investigate the effects of sky cuts on the low CMB multipoles using an estimator for which the estimator induced variance is demonstrably small.

2.2 PCL estimator

The PCL estimator is constructed from the spherical harmonic transform of the map

$$\tilde{a}_{\ell m} = \sum_i w_i \Delta T_i \Omega_i Y_{\ell m}(\theta_i), \quad (2)$$

where Ω_i is the solid angle of pixel i and w_i is a pixel weight function which henceforth will be set to unity for pixels outside the sky cut and to zero within the cut. From these spherical harmonic coefficients we can construct an unbiased estimator of the power spectrum,

$$\hat{C}_\ell^p = M_{\ell\ell'}^{-1} \tilde{C}_{\ell'}^p, \quad \tilde{C}_\ell^p = \frac{1}{(2\ell + 1)} \sum_m |\tilde{a}_{\ell m}|^2, \quad (3)$$

where M is a coupling matrix which can be expressed in terms of the power spectrum of the weight function w_i and 3-j coefficients (see Hivon *et al.* 2001). Analytic expressions for the covariance matrix of the PCL estimator accurate at high multipoles are given by Hinshaw *et al.* (2003), Chon *et al.* (2003) and E03c, and at low multipoles by E03c.

As is well known, the PCL estimator is sub-optimal and the estimator induced variance increases as the sky cut is increased, though for modest sky cuts (removing, say, 15 % of the sky), the estimator induced variance is small in comparison to the cosmic variance of the concordance Λ CDM cosmology (E03c). The analysis of the low CMB multipoles discussed by Hinshaw *et al.* (2003) uses the PCL estimator, \hat{C}_ℓ^p , of equation (3).

2.3 QML estimator

The QML estimator (Tegmark 1997) in the limit of negligible instrumental noise is

$$y_\ell = x_i x_j E_{ij}^\ell, \quad (4a)$$

where x_i is the data vector. (In the application discussed in this paper, the data vector consists of the temperature differences ΔT_i over the unmasked sky). The matrix E^ℓ in equation (4a) is

$$E^\ell = \frac{1}{2} C^{-1} \frac{\partial C}{\partial C_\ell} C^{-1}, \quad (4b)$$

where C is the covariance matrix $\langle x_i x_j \rangle$. The covariance matrix of the estimates y_ℓ is given by

$$F_{\ell\ell'} = \langle y_\ell y_{\ell'} \rangle - \langle y_\ell \rangle \langle y_{\ell'} \rangle = 2 \text{Tr} \left[C E^\ell C E^{\ell'} \right], \quad (5)$$

(Tegmark 1997).

From the estimates (4a), we can form an unbiased estimate of the CMB power spectrum

$$\hat{C}_\ell^q = F_{\ell\ell'}^{-1} y_{\ell'}, \quad (6)$$

with covariance matrix

$$\langle \Delta \hat{C}_\ell^q \Delta \hat{C}_{\ell'}^q \rangle = F_{\ell\ell'}^{-1}. \quad (7)$$

Table 1: Estimates of Estimator Induced Variance from Simulations

ΔT_ℓ^2	QML						PCL					
	all		< 1000	< 500	< 250	< 1000	all		< 1000	< 500	< 250	< 1000
	$\ell = 2$	$\ell = 3$	$\ell = 2$	$\ell = 2$	$\ell = 2$	$\ell = 3$	$\ell = 2$	$\ell = 3$	$\ell = 2$	$\ell = 2$	$\ell = 2$	$\ell = 3$
Kp2	45	50	32	26	18	41	244	203	134	84	55	132
Kp0	95	91	65	51	37	71	355	283	190	116	75	181

Notes to Table 1: The entries list the *rms* differences (in $(\mu K)^2$) between the estimated and input quadrupole and octopole amplitudes determined from 5000 simulations with the WMAP Kp2 and Kp0 sky masks. The columns marked ‘all’ show the results from all 5000 simulations. The remaining columns list the results with various restrictions placed on the amplitudes of the quadrupole and octopole in the simulations (see text for details).

The behaviour of the estimator (6) in the limit of low multipoles has been discussed by E03c. Let the data vector x_i consist of the harmonic coefficients $\tilde{a}_{\ell m}$ defined in equation (2). These coefficients are related to the true $a_{\ell m}$ coefficients on the uncut sky by a coupling matrix K ,

$$\tilde{a}_{\ell m} = \sum_{\ell' m'} a_{\ell' m'} K_{\ell m \ell' m'}. \quad (8)$$

If some of the sky is removed by a sky cut, the matrix K in equation (8) will be singular. This simply expresses the fact that there is no information on anisotropies that lie within the sky cut, hence it is impossible to reconstruct all of the $a_{\ell m}$ from the harmonic coefficients $\tilde{a}_{\ell m}$ measured on the cut sky. For small sky cuts and low multipoles, however, it may be a good approximation simply to truncate the summation in (8) at finite values of ℓ' and m' . The true low multipole coefficients $a_{\ell m}$ can then be reconstructed by inverting the non-singular truncated matrix \tilde{K} . In this case, the QML estimator becomes

$$\hat{C}_\ell^q \approx \frac{1}{(2\ell+1)} \sum_m |a_{\ell m}|^2, \quad a = \tilde{K}^{-1} \tilde{a}, \quad (9)$$

and is independent of the assumed form for the true power spectrum. (The variance on these estimates, is given by the cosmic variance of equation (1) and does, of course, depend on the assumed form for the input power spectrum).

The implication of the above analysis is that for small sky cuts, it is possible to reconstruct the exact power spectrum coefficients for our particular realisation of the sky using a QML estimator. In other words, estimator induced variance can be reduced to negligible levels if a QML estimator is used to estimate the low multipoles, provided the sky cut is small enough.

2.4 Simulations of Estimator Induced Variance

Equation (9) is approximate and will not apply for a large sky cut. How large does the sky cut have to be for equation (9) to break down? As a rough rule of thumb, equation (9) will be approximately correct if the the angular correlation function $C(\theta)$ can be estimated on the cut sky on all angular scales (Mortlock, Challinor and Hobson 2002). However, for a more precise assessment, the results of several sets of numerical simulations are describe in this sub-section. (Similar simulations are described in E03c).

A set of 5000 noise-free Gaussian CMB maps were generated using the igloo pixelization scheme described in E03c.

The input CMB power spectrum for these simulations is that of a simple six parameter Λ CDM model that provides an excellent fit to the WMAP power spectrum. This model will be referred to as the ‘fiducial Λ CDM model’ in this paper. The values of the six parameters of are given in E03b. A pixel size of $\theta_c = 5^\circ$ was used and the maps smoothed with a Gaussian beam of FWHM 7° . The WMAP Kp2 and Kp0 masks (see B03b for a discussion of the WMAP masks) were repixelised from the HEALPIX NSIDE=512 format (see Górski *et al.* 1999) onto the $\theta_c = 5^\circ$ igloo pixelization. The PCL and QML estimators, as described in the preceding sections, were then applied to each of the simulated maps after masking first by the Kp2 mask (which removes 17% of the sky at this resolution, see Figure 4b) and then by the Kp0 mask (which removes 25% of the sky, see Figure 4c).

Table 1 lists the *rms* differences between the estimated octopole and quadrupole amplitudes^{*}, ΔT_ℓ^2 and the true amplitudes, $(\Delta T_\ell^2)^T$, for the QML and PCL estimators. The numbers under the columns marked ‘all’ show the results for all 5000 simulations. For the Kp0 mask, the estimator induced variance of the PCL estimator at low multipoles is comparable to the cosmic variance for the fiducial Λ CDM model ($721 (\mu K)^2$ for the quadrupole and $567 (\mu K)^2$ for the octopole). Evidently, the Kp0 mask is close to the transition point at which the PCL estimator breaks down. The remaining entries in the table list the *rms* differences with various restrictions on the input quadrupole and octopole amplitudes of the simulations. Thus, Table 1 lists the differences if the input quadrupole amplitude is restricted to be less than $1000 (\mu K)^2$, $500 (\mu K)^2$ and $250 (\mu K)^2$, and if the octopole amplitude is restricted to be less than $1000 (\mu K)^2$. In all cases, estimator induced variance for the PCL estimator is several times larger than for the QML estimator. The results with the restrictions $(\Delta T_2^2)^T < 250 (\mu K)^2$ and $(\Delta T_3^2)^T < 1000 (\mu K)^2$ should give reasonable indications of the estimator induced variance, since these limits are close to the actual measured values of the octopole and quadrupole amplitudes (see Section 3).

The *rms* differences listed in Table 1 give a misleadingly favourable impression of the performance of the PCL

* Throughout this paper the amplitudes of the CMB multipoles will be expressed as

$$\Delta T_\ell^2 = \frac{1}{2\pi} \ell(\ell+1) C_\ell.$$

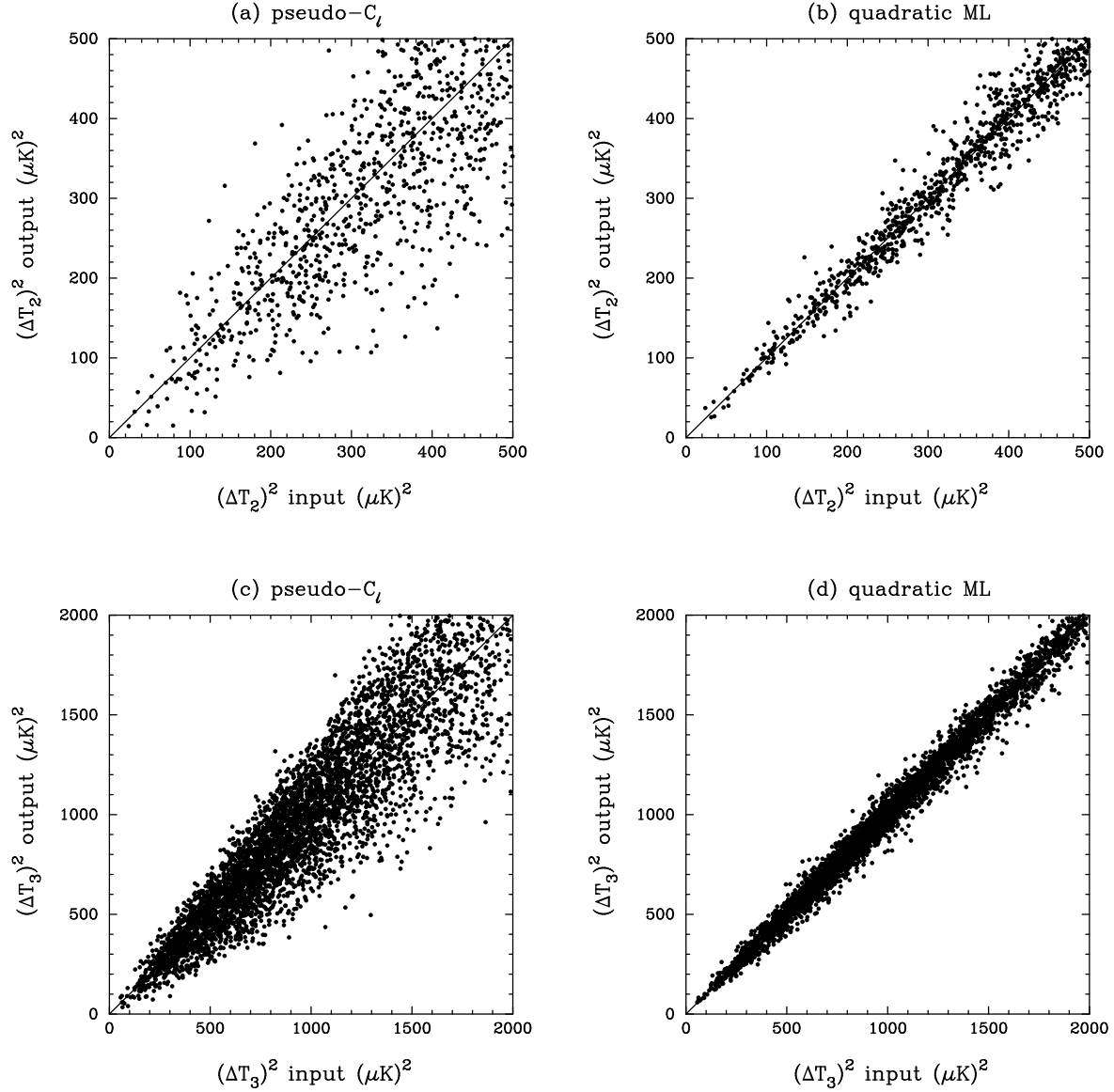


Figure 2. Comparison of the PCL and QML estimates of the quadrupole and octopole from simulations with the Kp2 mask. The abscissae list the input values of the quadrupole and octopole used to generate the simulated skies. The ordinates give the output values from the PCL estimator (Figures 2a and 2c) and QML estimator (Figures 2b and 2d) after the application of the Kp2 mask.

estimator because the distribution of the differences is non-Gaussian. This is illustrated by Figures 2 and 3 which show the estimated octopole and quadrupole amplitudes plotted against the input amplitudes for both estimators. Figure 2 shows the results for the simulations with the Kp2 mask and Figure 3 shows the results for the Kp0 mask. In particular, Figure 3a, shows how poorly the PCL estimator behaves when applied to simulations with the Kp0 mask. Here there are several examples of simulations with estimated quadrupole amplitudes of $\Delta T_2^2 \approx 100 (\mu K)^2$ where the true quadrupole amplitude is greater than $300 (\mu K)^2$. In contrast, the estimator induced variance for the QML is much smaller and more closely Gaussian distributed with a dispersion of $\approx 40 (\mu K)^2$. The estimator induced variance

for the QML estimator is almost a factor of two smaller in the simulations with the Kp2 mask and for most purposes can be ignored.

The results of this Section have quantified, by direct numerical simulation, the effects of estimator induced variance on QML and PCL estimators. As expected, when applied to maps with identical sky cuts the QML estimator gives much more accurate estimates of the low multipoles than the PCL estimator. For the Kp0 mask, which removes 25% of the sky, the estimator induced dispersion of the quadrupole amplitude is comparable to the actual measured value of the quadrupole. If one applied a mask that removed, contiguously, an even larger number of pixels than the Kp0 mask, the PCL estimator induced dispersion of the quadrupole am-

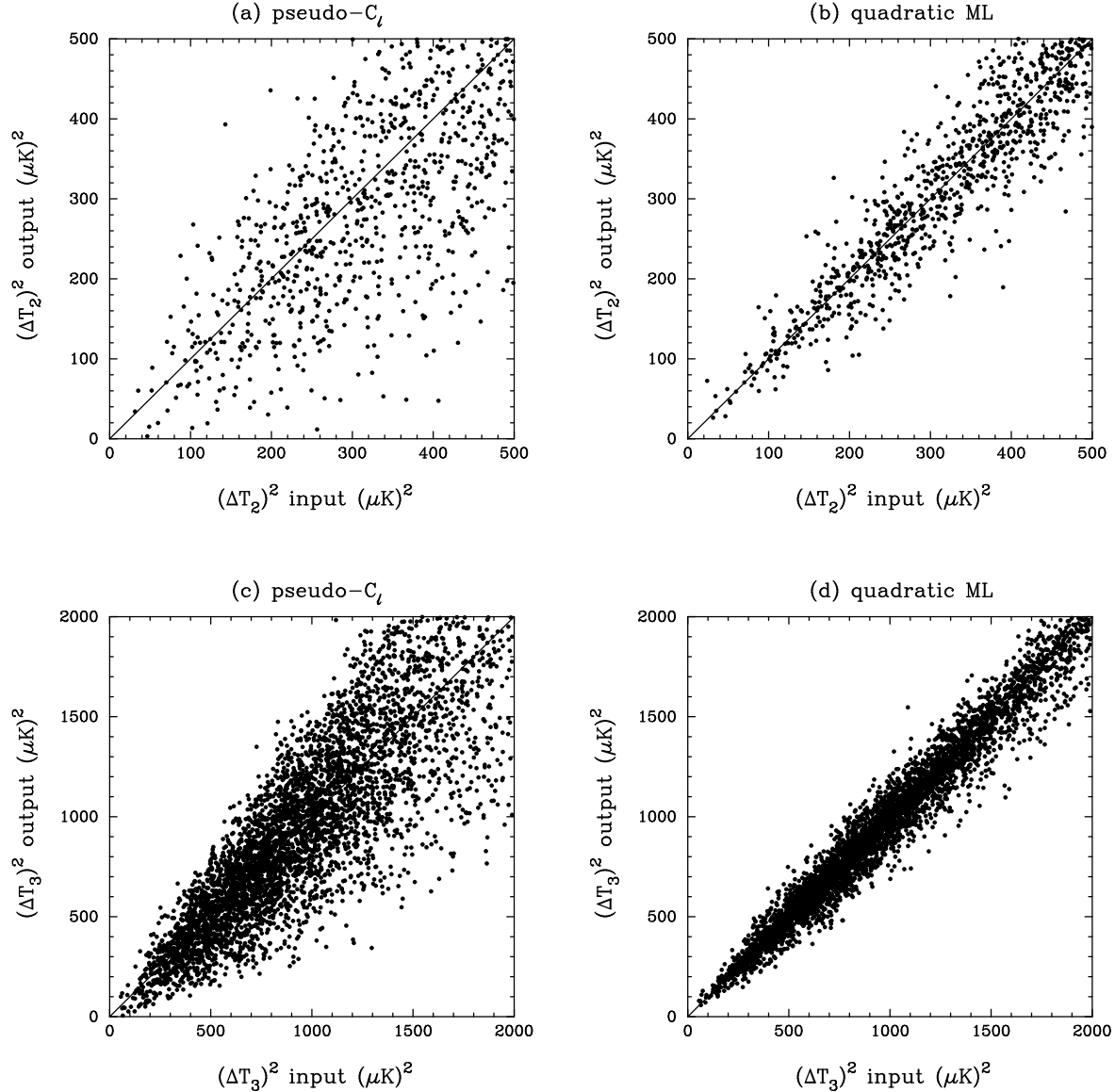


Figure 3. As Figure 2, but for simulations with the Kp0 mask.

plitude would become larger than the signal. In contrast, the estimator induced variance for the QML estimator is negligible for the Kp2 mask, and contributes a dispersion of about $40 (\mu K)^2$ for the quadrupole if the Kp0 mask is imposed.

Before applying the QML and PCL estimators to the WMAP component separated maps of Figure 1, it is worth anticipating some of the results:

(i) *Analysis of all sky component separated maps:* If the PCL and QML estimators are applied to all sky maps, the two estimators should give identical results because in this limit they are mathematically equivalent. Any differences between the estimated power spectrum and the primordial power spectrum for our realisation of the sky must then be caused by systematic errors. The differences between the power spectra estimated from the WMAP-ILC and TdOH03

maps would provide some indication of the effects of inaccurate subtraction of Galactic emission.

(ii) *Analysis of component separated maps with the Kp2 mask:* The estimator induced variance for the QML estimator is negligible in this case, hence any differences with the results from the all sky maps, or between the WMAP-ILC and TdOH03 maps, are likely to be caused by inaccurate subtraction of Galactic emission. Differences between the QML and PCL estimators will indicate the effects of estimator induced variance in the PCL estimates.

(iii) *Analysis of component separated maps with the Kp0 mask:* Small differences between the QML estimates applied to maps with the Kp0 mask and Kp2 masks could be caused by residual Galactic contamination or by estimator induced variance. Any differences will be consistent with estima-

tor induced variance if they are of order $40 (\mu K)^2$ for the quadrupole and of order $100 (\mu K)^2$ for the octopole. With the Kp0 mask, it would not be surprising to find large difference between the PCL and QML estimates, since the estimator induced variance for the PCL estimates is expected to be comparable to the measured amplitudes.

3 APPLICATION TO WMAP

3.1 Low resolution input maps and masks

The high resolution maps of Figure 1 were first degraded to a pixel size of $\theta_c = 5^\circ$ as follows. The harmonic coefficients $a_{\ell m}$ for the maps were computed by applying a spherical harmonic transform. The low resolution maps were then synthesised from the $a_{\ell m}$ (discarding the $\ell = 0$ and $\ell = 1$ multipoles) after multiplying by a Gaussian beam function of 7° FWHM. The low resolution maps are therefore equivalent in pixel size and resolution to the simulations described in the previous Section. The reduction in resolution is required so that the QML estimator, which requires of $\mathcal{O}(N_{\text{pix}})^3$ operations to evaluate, can be computed quickly. The $\theta_c = 5^\circ$ igloo pixelized maps contain $N_{\text{pix}} = 1632$ pixels,

The temperature differences of the low resolution WMAP-ILC and TdOH03 maps are plotted in Figure 4a. Differences are clearly apparent towards the Galactic plane and in the region of the Ophiucus complex (*cf* Figure 4 of Bennett *et al.* 2003a). Despite the obvious differences at low Galactic latitudes, the *rms* temperature differences between these two maps is only $8.9 \mu K$. For comparison the *rms* temperature anisotropy of the WMAP-ILC map at this resolution is $40.3 \mu K$. The Kp2 and Kp0 masks are shown in Figures 4b and 4c. Most of the discrepant pixels in Figure 4a are eliminated by the Kp2 mask. Even with the Kp0 mask, however, there are residual differences between the two maps (the *rms* temperature differences for pixels outside the Kp0 mask is $5.6 \mu K$, see Table 2). Figure 4d shows a more extensive mask (denoted Kp0+) which consists of the Kp0 mask and those pixels in the difference map that differ by more than $8.2 \mu K$ ($\Delta T/T = 3 \times 10^{-6}$). Some of the additional masked pixels, for example, in the region of Orion, may reflect inaccuracies in Galactic subtraction. However, most of the differences at high Galactic latitude correlate with regions of high emission in the component separated maps (Figure 1). These differences are most likely caused by small differences in the way that the two component separated maps were constructed (for example, differences in smoothing of the individual frequency maps) rather than by low level Galactic emission. Nevertheless, it is interesting to investigate the effects on the low CMB multipoles by applying the Kp0+ mask.

3.2 Amplitudes of the Low CMB Multipoles

The power spectra, up to a multipole of $\ell = 20$, for the four masks of Figure 4, are plotted in Figures 5 and 6. Figure 5 shows the results for the WMAP-ILC map and Figure 6 shows the results for the TdOH3 map. In each plot the solid lines show the results from the PCL estimator (equation 3) and the filled circles show the results of the QML estimator (equation 6). The error bars on the QML points are

computed from the diagonal components of the covariance matrix (equation (7) assuming the fiducial Λ CDM model).

In the case of no mask the QML and PCL estimates are identical, as expected. However, the estimators differ when applied to the masked maps. Given the discussion in Section 2.4, we would expect the QML estimates to remain relatively stable as more of the sky is masked. The PCL estimator is expected to show larger changes as more of the sky is masked because of the increasing importance of estimator induced variance. This is exactly what is seen in Figures 5 and 6.

The amplitudes of the quadrupole and octopole for the four masks are listed in Table 2. For reference, the amplitudes listed in the WMAP public data release (see also Table 3) are $\Delta T_2^2 = 123 (\mu K)^2$ and $\Delta T_3^2 = 611 (\mu K)^2$. These numbers were determined by applying a PCL estimate to the V and W band maps with the Kp2 mask (Hinshaw *et al.* 2003) and are quite close the PCL estimates for the WMAP-ILC map listed in Table 2 ($\Delta T_2^2 = 116 (\mu K)^2$, $\Delta T_3^2 = 480 (\mu K)^2$). The quadrupole and octopole amplitudes in the case of no mask are almost identical with the PCL amplitudes estimated by TdOH03 from the two component separated maps. For both maps, the QML quadrupole amplitude is relatively stable as more of the sky is masked. For example, for the WMAP-ILC map the QML quadrupole amplitude varies from $192 (\mu K)^2$ for no mask to $176 (\mu K)^2$ for the Kp0 mask. In contrast, the PCL quadrupole amplitude halves from $194 (\mu K)^2$ for no mask to $97 (\mu K)^2$ for the Kp0 mask. The discussion in Section 2.4 shows that differences of this order are consistent with the PCL estimator induced variance. *The QML estimates, which are stable for different masks, provide more reliable estimates.*

Similar remarks apply to the analysis of the TdOH03 map. The differences between the QML estimates for the WMAP-ILC and TdOH03 maps provides some indication of the effects of inaccurate subtraction of Galactic emission. For the Kp2 mask, the difference in quadrupole amplitudes is $27 (\mu K)^2$ and this rises to $69 (\mu K)^2$ for the Kp0 mask. These differences are broadly compatible with the estimate given in Bennett *et al.* (2003a) that the 95% uncertainty in the quadrupole amplitude caused by modelling Galactic foregrounds is about $70 (\mu K)^2$. Notice that applying the QML estimates for the more conservative Kp0+ mask are almost identical to the estimates for the Kp0 mask (*cf* Figures 5 and 6). (This is not surprising because most of the additional masked pixels in the Kp0+ mask are not contiguous with the Kp0 mask.)

Which of these estimates is likely to be the most reliable? The simulations in Section 2.4 suggest that the results for the Kp2 mask are likely to be the most accurate. Clearly, the largest differences between the WMAP-ILC and TdOH3 maps lie within the Kp2 mask, and since we have demonstrated that the estimator induced variance with the Kp2 mask is small, the Kp2 QML estimates are more likely to be accurate than the estimates from the unmasked maps. The differences between the Kp2 estimates for the two component subtracted maps then provide some indications of the effects of inaccuracies in subtracting Galactic emission. The QML estimator induced variance does begin to become important for the Kp0 mask. The small differences between the QML results for the Kp2 and Kp0 masks are more likely to be caused by estimator induced variance than to errors in Galactic subtraction (*cf* Figures 2 and 3).

Table 2: Amplitudes of the Quadrupole and Octopole from WMAP

mask	f_{sky}	σ_{maps}	WMAP-ILC				TdOH03			
			QML		PCL		QML		PCL	
			ΔT_2^2	ΔT_3^2	ΔT_2^2	ΔT_3^2	ΔT_2^2	ΔT_3^2	ΔT_2^2	ΔT_3^2
0	1.00	8.9	192	1039	194	1052	198	852	201	865
Kp2	0.83	6.2	223	1183	116	480	250	1081	154	471
Kp0	0.75	5.6	176	805	97	325	245	794	142	331
Kp0+	0.64	4.1	182	817	120	289	231	804	145	292

Notes to Table 2: The second column lists the fraction of sky that is unmasked. The third column (labelled σ_{maps}) lists the *rms* temperature difference in μK of the WMAP-ILC and TdOH03 maps in the unmasked region of the sky. The remaining columns list the quadrupole and octopole amplitudes in $(\mu K)^2$ determined from the QML and PCL estimators.

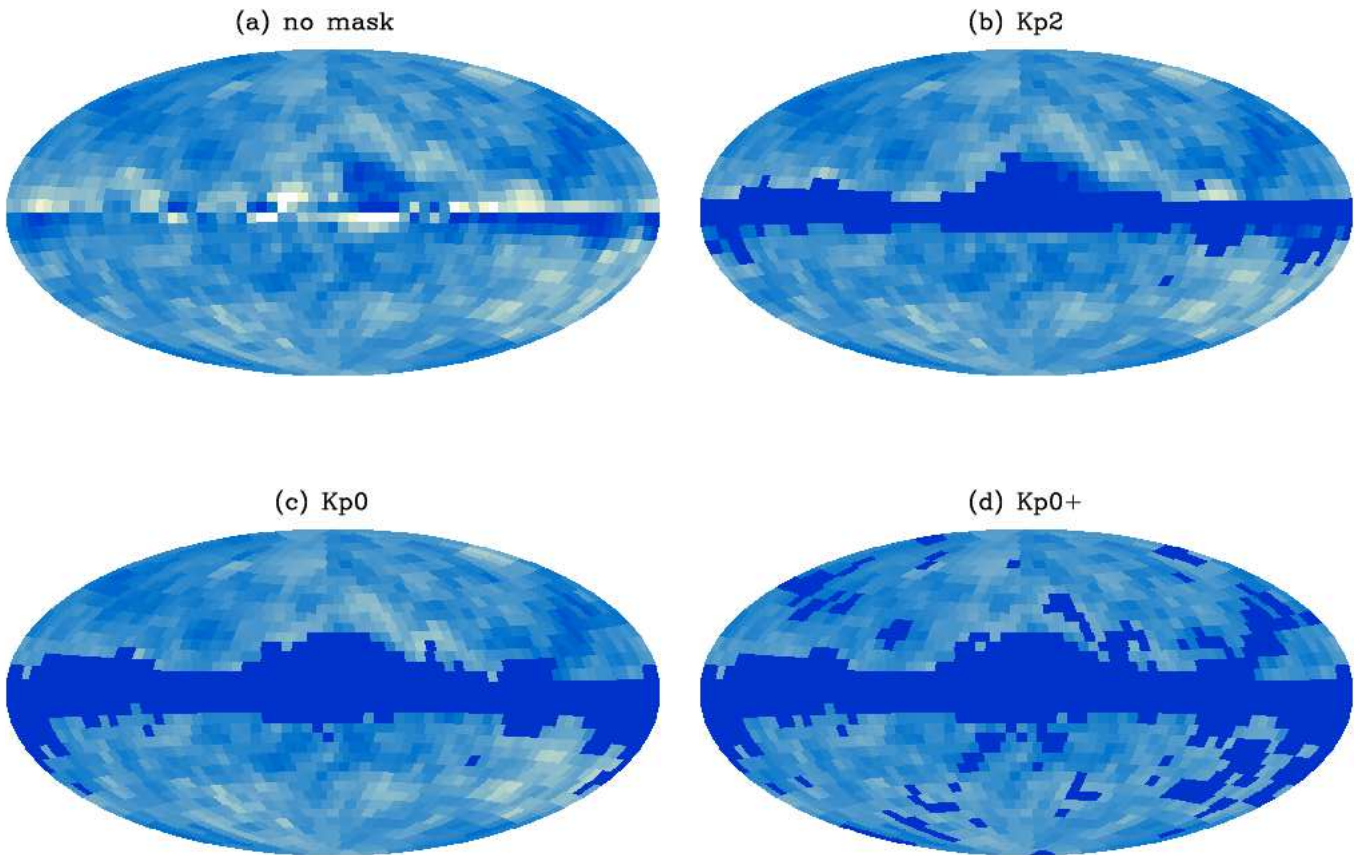


Figure 4. Temperature differences of the low resolution WMAP-ILC and TdOH03 maps. Figure 4a shows the whole sky, for which the *rms* temperature difference is $8.9\mu K$. The Kp2 and Kp0 masks are shown in figures 4b and 4c. Figure 4d shows the Kp0+ mask defined in the text, which consists of the Kp0 mask and those pixels for which the temperature difference between the two maps differs by more than $\Delta T/T = 3 \times 10^{-6}$ ($8.2\mu K$).

The QML estimates for the first 20 CMB multipoles with the Kp2 mask are listed in Table 3. The PCL amplitudes estimated by the WMAP team are also listed in Table 3 for comparison. The errors on the QML estimates are computed from the diagonal components of the covariance matrix assuming the fiducial Λ CDM model. Since the estimator induced variance for the Kp2 mask is small, the

covariance matrix is very accurately diagonal (see the plots of the Fisher matrix in Figures 5 and 6), and the error estimates are very close to the cosmic variance errors (equation 1). The errors on the WMAP estimates are computed from equation (13) of Verde *et al.* (2003) assuming the fiducial Λ CDM model.

The difference between the two sets of QML estimates

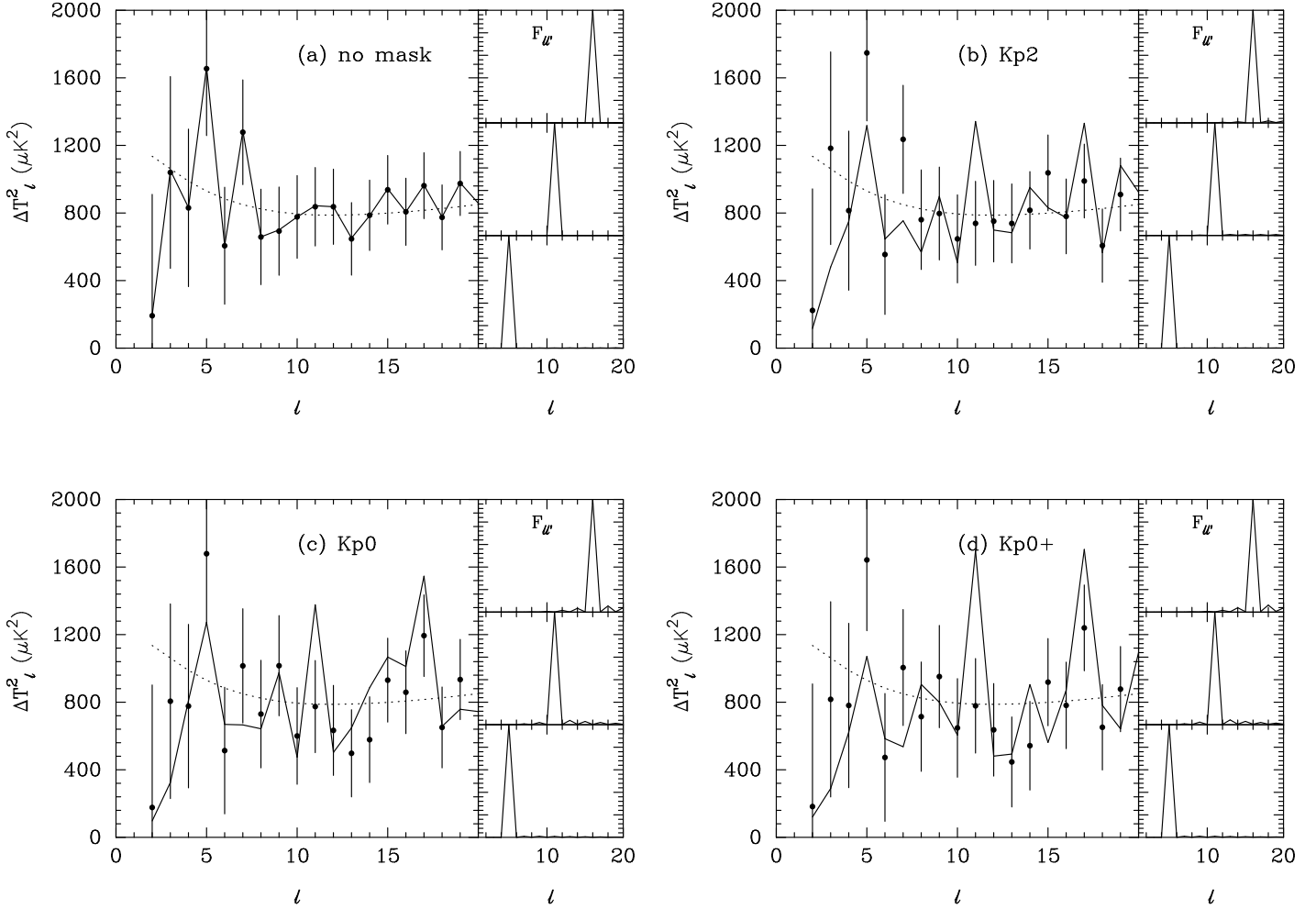


Figure 5. The low CMB multipoles computed from the WMAP-ILC map. The filled circles show the QML estimates of ΔT_ℓ^2 and the solid lines show the PCL estimates. The error bars on the points are computed from the diagonal components of the Fisher matrix $F_{\ell\ell}$, which assumes the fiducial Λ CDM model. The panels to the right show three rows of the Fisher matrix. Figure 5a shows the results if no Galactic mask is imposed. The Kp2 Galactic mask is used for Figure 5b, the Kp0 mask for Figure 5c, and the Kp0+ mask for Figure 5d. The dotted lines show the power spectrum of the fiducial Λ CDM model.

in Table 3 provide some indications of the effects of inaccuracies in subtraction of Galactic emission. The *rms* difference in the estimates from $\ell = 10$ to $\ell = 20$ is $88(\mu K)^2$. This is compatible with the 5 – 10% variations at low multipoles seen in the cross power spectra of the external template foreground subtracted Q, V and W maps (see Figure 3 of Hinshaw *et al.* 2003). In agreement with the WMAP team’s conclusions, these tests suggest that inaccuracies in foreground subtraction are substantially smaller than the cosmic variance at low multipoles. They are not, however, negligible and should be included in detailed analyses (*e.g.* assessing the statistical significance of the quadrupole discrepancy, *cf* TdOH03, E03b).

3.3 Implications for the concordance Λ CDM cosmology.

The results from the QML estimator presented in the preceding sub-section shows that WMAP estimate of the

quadrupole amplitude of $123(\mu K)^2$ is an underestimate of the true value, which is more likely to be about $200(\mu K)^2$. Table 4 lists the probability P of finding a quadrupole amplitude smaller than the observed value in the fiducial Λ CDM model. The first row of Table 4 lists P for the WMAP PCL estimates of Hinshaw *et al.* (2003). This was computed by applying the PCL estimator to simulated CMB skies with the Kp2 mask and so includes estimator induced variance. The remaining entries list the probabilities for the QML estimates computed from equation (3) of E03b (*i.e.* assuming a χ^2 distribution with cosmic variance). These are consistently higher than the value of P for the PCL estimate. There is no discrepancy here. Since the PCL estimator is inferior to the QML estimator, the frequentist probability P computed for the PCL estimator from a single realization of the sky will be less reliable than the frequentist probability determined from the QML estimator. The results of Table 4 are in agreement with those of TdOH03 and E03b. If the concordance Λ CDM model is correct, the probability P is

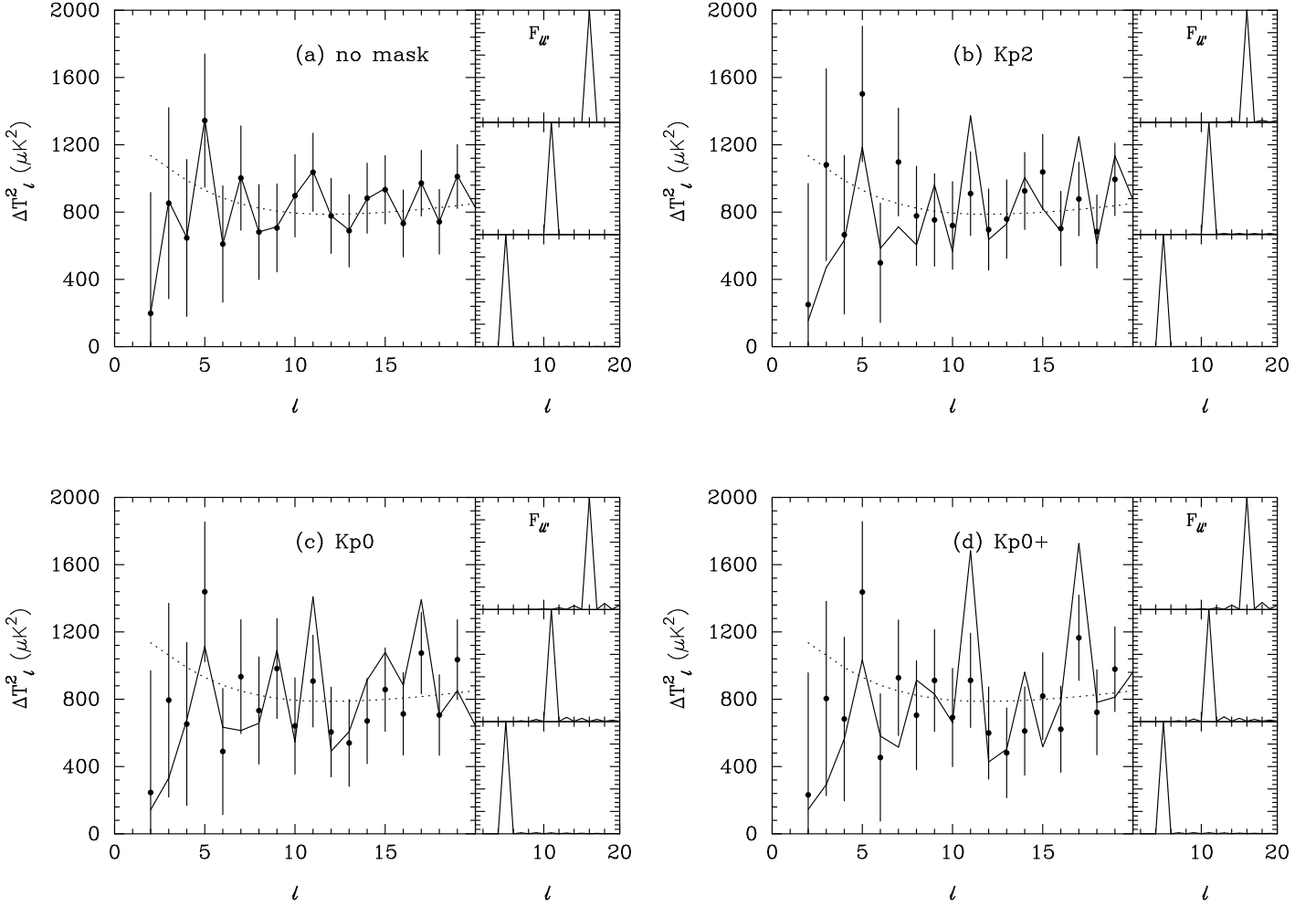


Figure 6. As Figure 5, but for the component separated map of TdOH03.

in the region of 2.5% – 4.5% depending on which component separated map is used. Similar remarks apply to the QML octopole amplitudes given in Table 2. The analysis described here reinforces the conclusion of a previous paper (E03b) that the discrepancy with the concordance Λ CDM model at low multipoles is of order a few percent rather than at the 0.15% level argued by Spergel *et al.* (2003).

4 ANGULAR CORRELATION FUNCTION AND THE S STATISTIC

SO3 quantified the lack of structure in the CMB sky on large angular scales by evaluating the statistic

$$S = \int_{-1}^{1/2} [C(\theta)]^2 d \cos \theta, \quad (10)$$

where $C(\theta)$ is the angular correlation function computed from the PCL estimates of the power spectrum C_ℓ ,

$$C(\theta) = \frac{1}{4\pi} \sum (2\ell + 1) C_\ell P_\ell(\cos \theta). \quad (11)$$

By comparing values of S determined from a large number of simulations generated from the posterior distribution of the Λ CDM cosmology (using the same sky cut and estimator as for the real data) they concluded that the probability of finding a value of S smaller than that observed is about 0.15%.

The integration limits for the S statistic ($\theta > 60^\circ$) were chosen a posteriori to correspond to the angular scales over which the measured $C(\theta)$ is close to zero. Over these angular scales the quadrupole and octopole make significant contributions to the sum in (11) but the next few multipoles also make some contribution. The statistic S is thus not equivalent to a test based on the amplitudes of the quadrupole and octopole anisotropies alone. It is therefore interesting to analyse the S statistic using an optimal estimate of the power spectrum in equation (11) and to contrast this analysis with the results of Table 4.

Evidently, the S statistic will show estimator induced variance since it is constructed from estimates of the power spectrum. As with the power spectrum estimates discussed in Section 2.2, the estimator induced variance of the S statistic applied to a cut sky will be higher if a PCL estimate of

Table 3: Comparison of QML estimates and errors for the Kp2 mask with published WMAP estimates and errors

ℓ	ΔT_ℓ^2		
	WMAP (PCL)	TdOH03 (QML)	WMAP-ILC (QML)
2	123 ± 845	250	223 ± 720
3	611 ± 667	1081	1183 ± 570
4	756 ± 548	665	813 ± 471
5	1257 ± 466	1502	1748 ± 402
6	696 ± 407	498	554 ± 355
7	830 ± 364	1097	1236 ± 319
8	627 ± 332	777	760 ± 294
9	815 ± 307	753	797 ± 274
10	617 ± 288	720	647 ± 260
11	1251 ± 273	910	739 ± 248
12	759 ± 261	696	751 ± 241
13	714 ± 252	758	738 ± 233
14	907 ± 245	925	816 ± 229
15	871 ± 238	1038	1037 ± 224
16	628 ± 234	701	780 ± 221
17	1042 ± 229	878	989 ± 218
18	742 ± 226	684	607 ± 217
19	947 ± 223	994	909 ± 215
20	870 ± 221	715	782 ± 214

Notes to Table 3: The second column lists the amplitudes of the low order CMB multipoles from the WMAP public data release, which uses a PCL estimator and the Kp2 mask. The errors on these numbers are given by equation (13) of Verde *et al.* (2003) assuming the fiducial Λ CDM model. The second and third columns list the QML estimates for the TdOH03 and WMAP-ILC maps with the Kp2 mask applied. The errors on the QML estimates (which are identical for both maps) are computed from the diagonal components of the covariance matrix (equation (7) assuming the fiducial Λ CDM model).

Table 4: Significance of quadrupole discrepancy

method	map	mask	ΔT_2^2	P
PCL	(WMAP analysis)	Kp2	123	1.3%
QML	WMAP-ILC	0	192	2.6%
QML	TdOH03	0	198	2.8%
QML	WMAP-ILC	Kp2	223	3.6%
QML	TdOH03	Kp2	250	4.5%
QML	WMAP-ILC	Kp0	176	2.1%
QML	TdOH03	Kp0	245	4.4%

C_ℓ is used in the sum (11) than if a QML estimate is used. This is illustrated in Figure 7 which compares input and output values of the S statistic determined from simulated skies with the Kp2 cut applied using PCL (Figure 7a) and QML (Figure 7b) estimates of the power spectrum. estimates)[†].

[†] Note that a direct determination of $C(\theta)$ by summing over pixels on a cut sky (say as in Gaztañaga *et al.*, 2003) will have similar estimator induced variance as the summation (11) using a PCL estimator.

Table 5: Significance of the S statistic

method	map	mask	S	$P(S < S_{\Lambda\text{CDM}})$
PCL	(WMAP analysis)	Kp2	1644.	0.18%
QML	WMAP-ILC	0	7891	6.9%
QML	TdOH03	0	4995	3.2%
QML	WMAP-ILC	Kp2	11437	12.5%
QML	TdOH03	Kp2	9929	9.7%
QML	WMAP-ILC	Kp0	5365	3.9%
QML	TdOH03	Kp0	5108	3.7%

Notes to Table 5: A comparison of values of the S statistic (equation 10) and its statistical significance. The first row gives the results for the publically released WMAP PCL estimates listed in Table 3. The remaining rows list results using QML estimates of the power spectrum for various sky cuts. The fourth column list the value of S (in units of $(\mu K)^5$). The fifth column lists the frequency $P(S < S_{\Lambda\text{CDM}})$ of finding a value of S smaller than that observed if the fiducial Λ CDM model is correct.

For any given Galactic cut, a PCL-based S statistic will *always* be inferior to a QML-based S statistic. An analysis of a QML-based S statistic must therefore give a more accurate estimate of the statistical significance of the lack of structure in the CMB sky than the analysis described by SO3. Figure 8 shows the angular correlation function using the three power spectrum estimates listed in Table 3 evaluated with the Kp2 mask (WMAP PCL, TdOH03 QML and WMAP-ILC QML). Although all three estimates are close to zero on angular scales $90^\circ \lesssim \theta \lesssim 150^\circ$, the values of the S statistic differ significantly, as does the inferred statistical significance of a discrepancy with the fiducial Λ CDM model. Table 5 lists the values of S (in units of $(\mu K)^4$) inferred from the publically released PCL power spectrum estimates and also for QML estimates for various sky cuts. The final column of Table 5 lists the frequency $P(S < S_{\Lambda\text{CDM}})$ of finding a value smaller than the one observed if the fiducial Λ CDM model is correct. These frequencies were estimated directly from the simulated CMB skies, using identical estimators and sky cuts to those applied to the real data. All of the QML estimates give frequencies of a few percent, in qualitative agreement with the frequencies listed in Table 4.

Only the first row of Table 5, using the WMAP PCL estimates gives a low frequency of 0.18%. This low frequency is consistent with the analysis of SO3. It is also broadly consistent with the low frequency of 0.35% of finding a quadrupole *and* octopole amplitude lower than the WMAP PCL estimates given the fiducial Λ CDM model (E03b). However, since these frequencies are based on PCL estimates, they *must necessarily* be less reliable than the frequencies based on QML power spectrum estimates. In particular, the low frequency inferred by SO3 from the S statistic is simply an unfortunate consequence of the way that PCL estimator induced variance has affected estimates of the low CMB multipoles. The more reliable QML (or QML-based) estimates listed in Tables 4 and 5 show that a more accurate estimate of the significance level of the discrepancy with the fiducial Λ CDM model is of order a few percent.

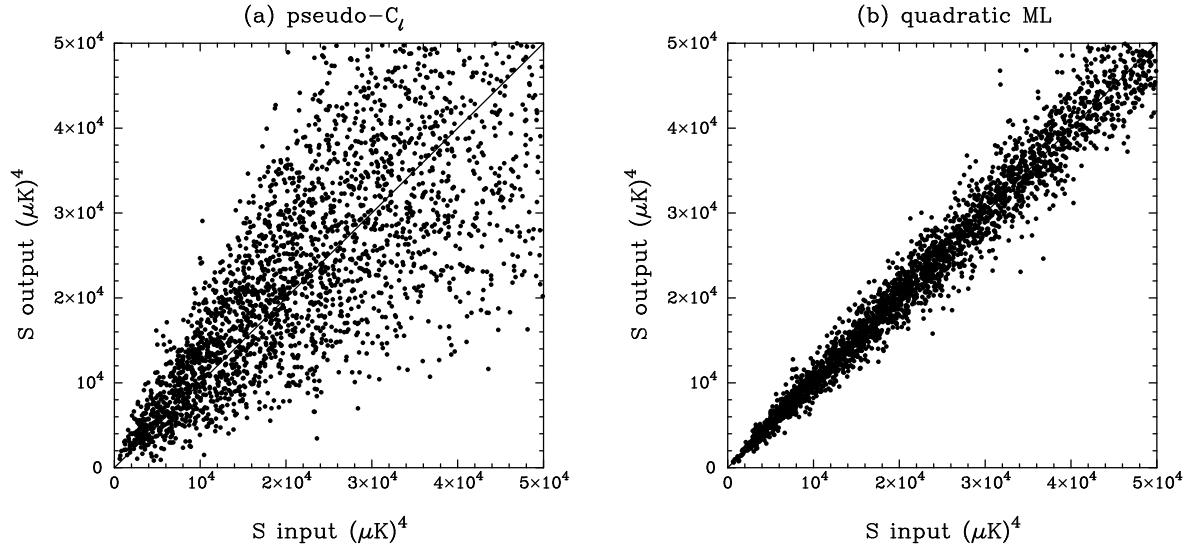


Figure 7. Comparison of the PCL and QML estimates of S statistic (equation 10) from simulations with the Kp2 mask. The abscissae list the values of the S statistic for the input simulated skies. The ordinates give the output values from the PCL estimator (Fig 7a) and QML estimator (Fig 7b) after the application of the Kp2 mask.

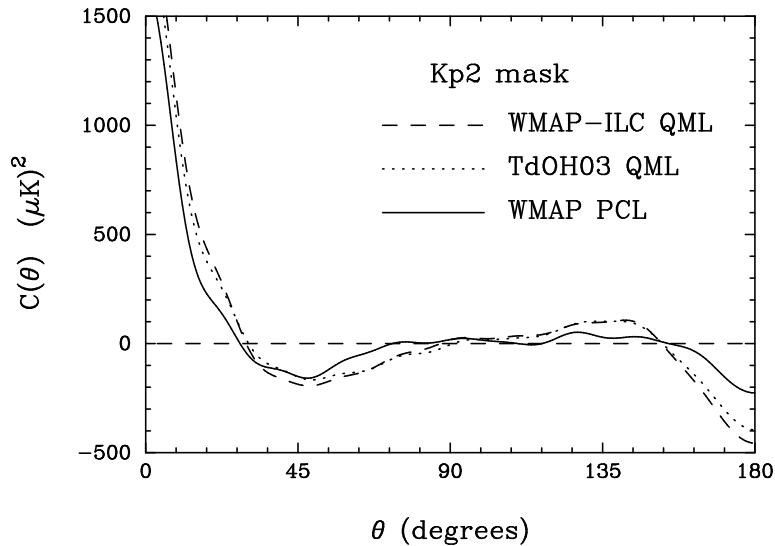


Figure 8. Estimates of the angular correlation function

5 CONCLUSIONS

In this paper, we have investigated the effects of sky cuts on PCL and QML estimators using numerical simulations. For QML estimators, the estimator induced variance of the quadrupole amplitude is less than $40 (\mu K)^2$ for the WMAP Kp0 mask and, for most purposes, is negligible when the less severe Kp2 mask is applied. In contrast, at low multipoles the PCL estimator begins to break down for the Kp0 mask, since the estimator induced dispersion for such a large sky cut is comparable to the signal. A QML estimator is therefore preferable to a PCL estimator, and for small enough sky cuts is capable of returning almost the exact amplitudes of the low multipoles for our realization of the CMB sky.

The PCL and QML estimators have been applied to the

Galaxy subtracted maps produced by B03b and TdOH03 to estimate the amplitudes of the CMB multipoles at $\ell \leq 20$. The QML estimates (in contrast to the PCL estimates) are found to be stable to the imposed Galactic cut. This stability, and the agreement between the power spectra from the two maps, suggests that inaccuracies in Galactic subtraction introduce errors of order 10% or less in the amplitudes of the low multipoles.

The QML quadrupole and octopole amplitudes are found to lie in the ranges $\Delta T_2^2 = 176 - 250 (\mu K)^2$ and $\Delta T_3^2 = 794 - 1183 (\mu K)^2$ and are more likely to lie at the upper ends of these ranges since these values correspond to the Kp2 Galactic cut, for which the estimator induced variance and Galactic emission is small. In contrast, the WMAP team

derived values $\Delta T_2^2 = 123 (\mu K)^2$ and $\Delta T_3^2 = 611 (\mu K)^2$ by applying a PCL estimator to maps with the Kp2 sky cut. There can be no question that the QML estimates are more reliable than the PCL estimates. There is, therefore, strong evidence that the discrepancy between the quadrupole and octopole amplitudes and those expected in the concordance Λ CDM model is considerably less significant than the 0.15% estimated by SO3. This is consistent with the analysis of the S statistic described in Section 4 using QML estimates. The results summarized in Tables 4 and 5, in fact suggest, a significance level of the low multipole discrepancy of a few percent.

The results described here are compatible with those of TdOH03. These authors derived quadrupole and octopole amplitudes of $\Delta T_2^2 = 202 (\mu K)^2$ and $\Delta T_3^2 = 856 (\mu K)^2$ (very close to the numbers given in Table 2) from an analysis of their all sky component separated map. They argued that the residual contamination from inaccurate Galactic subtraction was small enough, and confined to a sufficiently small number of pixels close to the Galactic plane, that the results of the all-sky analysis should give accurate estimates of the quadrupole and octopole amplitudes. This is consistent the analysis presented in this paper, since the QML estimates are found to be insensitive to the Galactic cut.

The results presented here weaken the case that any exotic new physics is required to explain the amplitudes of the low CMB multipoles.

Acknowledgments: I thank Max Tegmark for supplying copies of the TdOH03 maps and to various members of the Planck analysis group at Cambridge for useful discussions.

REFERENCES

- Bahcall N.A., Ostriker J.P., Perlmutter S., Steinhardt P.J., 1999, *Science*, 284, 1481.
- Bennett C.L. *et al.*, 2003a, *ApJS*, 148, 1.
- Bennett C.L. *et al.*, 2003b, *ApJS*, 148, 97.
- Bridle S.L., Lewis A.M., Weller J., Efstathiou G., 2003, *MNRAS*, 342, L72.
- Chon G., Challinor A., Prunet S., Hivon E., Szapudi I., 2003, *MNRAS*, in press. astro-ph/0303414.
- Cline J.M., Crotty P., Lesgourgues J., 2003, preprint. astro-ph/0304558.
- Contaldi C. Peloso M., Kofman L., Linde A., 2003, astro-ph/0303636.
- DeDeo S., Caldwell R.R., Steinhardt P.J. 2003, *PRD*, D67, 103509.
- Efstathiou G., 2003a, *MNRAS*, 343, L95.
- Efstathiou G., 2003b, *MNRAS* in press. astro-ph/0306431.
- Efstathiou G., 2003c, submitted to *MNRAS*. astro-ph/0307515.
- Feng B., Zhang X., 2003, preprint. astro-ph/0305020.
- Gaztañaga E., Wagg J., Multamaki T., Montana A., Hughes D.H., 2003, *MNRAS* in press. astro-ph/0304178.
- Hinshaw G. *et al.*, 2003, *ApJS*, 148, 135.
- Hivon E., Górski K.M., Netterfield C.B., Crill B.P., Prunet S., Hansen F., 2002, *ApJ*, 567, 2.
- Mortlock D.J., Challinor A.D., Hobson M.P., 2002, *MNRAS*, 330, 405.
- Niarchou A., Jaffe, A.H., Pogossian L., 2003, astro-ph/0308461.
- Peebles P.J.E., 1973, *ApJ*, 185, 431.
- Spergel D.N. *et al.*, 2003, *ApJS*, 148, 175.
- Tegmark M., 1997, *PRD*, 55, 5895.
- Tegmark M., Efstathiou G., 1996, *MNRAS*, 281, 1297.

- Tegmark M., de Oliveira-Costa A., Hamilton A., 2003, astro-ph/0302496.
- Verde L., *et al.*, 2003, *ApJS*, 148, 195.
- Wandelt B.D., Hivon E., Górski K.M., 2001, *PRD*, 64, 083003.
- Wang X., Tegmark M., Zaldarriaga M., 2002, *PRD*, 65, 123001.